J. Mt. Sci. (2023) 20(8): 2263-2281 e-mail: jms@imde.ac.cn http://jms.imde.ac.cn
https://doi.org/10.1007/s11629-022-7872-x

Original Article

Hydrological response under CMIP6 climate projection in Astore River Basin, Pakistan

Zeshan ALI[1,2] https://orcid.org/0000-0002-7175-4139; e-mail: engrzeshanali@yahoo.com

Mudassar IQBAL[1*] https://orcid.org/0000-0002-9310-5391; e-mail: mudassar@cewre.edu.pk

Ihsan Ullah KHAN[1] https://orcid.org/0000-0003-1139-6525; e-mail: ihsankhan4848@gmail.com

Muhammad Umer MASOOD[1] https://orcid.org/0000-0002-3085-7473; e-mail: umer.cewre@gmail.com

Muhammad UMER[3] https://orcid.org/0000-0002-9233-1485; e-mail: umer@rainbow.iis.u-tokyo.ac.jp

Muhammad Usama Khan LODHI[1] https://orcid.org/0000-0002-4168-8038; e-mail: mlodhi51@yahool.com

Muhammad Atiq Ur Rehman TARIQ[4*] https://orcid.org/0000-0002-0226-7310; e -mail: muhammadatiqurrehman.tariq@cdu.edu.au

**Corresponding author*

1 Centre of Excellence in Water Resources Engineering, University of Engineering and Technology, Lahore 54890, Pakistan

2 International Water Management Institute, Lahore 53700, Pakistan

3 Department of Civil Engineering, University of Tokyo, Tokyo 113-8656, Japan

4 Faculty of Science and Technology, Engineering, Charles Darwin University, Darwin, NT 0810, Australia

Citation: Ali Z, Iqbal M, Ullah Khan I, et al. (2023) Hydrological response under CMIP6 climate projection in Astore River Basin, Pakistan. Journal of Mountain Science 20(8). https://doi.org/10.1007/s11629-022-7872-x

© The Author(s) 2023

Abstract: Climate change strongly influences the available water resources in a watershed due to direct linkage of atmospheric driving forces and changes in watershed hydrological processes. Understanding how these climatic changes affect watershed hydrology is essential for human society and environmental processes. Coupled Model Intercomparison Project phase 6 (CMIP6) dataset of three GCM's (BCC-CSM2-MR, INM-CM5-0, and MPI-ESM1-2-HR) with resolution of 100 km has been analyzed to examine the projected changes in temperature and precipitation over the Astore catchment during 2020-2070. Bias correction method was used to reduce errors. In this study, statistical significance of trends was performed by using the Man- Kendall test. Sen's estimator determined the magnitude of the trend on both seasonal and annual scales at Rama Rattu and Astore stations. MPI-ESM1-2-HR showed better results with coefficient of determination (COD) ranging from 0.70-0.74 for precipitation and 0.90-0.92 for maximum and minimum temperature at Astore, Rama, and Rattu followed by INM-CM5-0 and BCC-CSM2-MR. University of British Columbia Watershed model was used to attain the future hydrological series and to analyze the hydrological response of Astore River Basin to climate change. Results revealed that by the end of the 2070s, average annual precipitation is projected to increase up to 26.55% under the SSP1-2.6, 6.91% under SSP2-4.5, and decrease up to 21.62% under the SSP5-8.5. Precipitation also showed

Received: 22-Dec-2022
Revised: 20-May-2023
Accepted: 09-Jun-2023

considerable variability during summer and winter. The projected temperature showed an increasing trend that may cause melting of glaciers. The projected increase in temperature ranges from -0.66°C to 0.50°C, 0.9°C to 1.5°C and 1.18°C to 2°C under the scenarios of SSP1-2.6, SSP2-4.5 and SSP5-8.5, respectively. Simulated streamflows presented a slight increase by all scenarios. Maximum streamflow was generated under SSP5-8.5 followed by SSP2-4.5 and SSP1-2.6. The snowmelt and groundwater contributions to streamflow have decreased whereas rainfall and glacier melt components have increased on the other hand. The projected streamflows (2020-2070) compared to the control period (1990-2014) showed a reduction of 3% - 11%, 2% - 9%, and 1% - 7% by SSP1-2.6, SSP2-4.5, and SSP5-8.5, respectively. The results revealed detailed insights into the performance of three GCMs, which can serve as a blueprint for regional policymaking and be expanded upon to establish adaption measures.

Keywords: GCMs; UBCWM; Astore River; Climate Change; Upper Indus Basin; Bias Correction

1 Introduction

Climate change (CC) is inextricably linked to the availability of catchment water resources. Climate change has a significant role in the transformation of the ecosystem and contributes to an increase in global warming (Zhang et al. 2017). It affect catchments through the explicit impact of atmospheric drivers (i.e., temperature, precipitation) and indistinguishable changes in hydrological processes (Iqbal et al. 2022). The 48th session of the Intergovernmental Panel on Climate Change (IPCC) agreed on a World Warming Special Report, and the global mean temperature increase could still be confined to 1.5°C (IPCC 2021). According to the sixth Intergovernmental Panel on Climate Change IPCC Assessment Report 6 that climate change is accelerating, and its impacts may become more extreme in the future. Archer et al. (2010) concluded that water resources sustainability appears to be more vulnerable to socio-economic changes than to climatic trend. Pakistan is highly dependent on surface water because it is an agriculture based economy. The Indus River system irrigate most fertile land of Pakistan. Water is, therefore, the lifeline for its food security and economic growth, both of which depend upon the suitable and appropriate availability of water. With a rapidly growing population, there is tremendous stress on water resources. In Pakistan, per capita availability of water is declined with the passage of time because of combined impact of increasing population, decreasing streamflow, and reduced reservoir storage capacities (Tahir et al. 2016). The susceptibility of the hydrology of the Upper Indus Basin (UIB) to climate change is well-established, as studies have shown that significant increases in air temperature can lead to changes in water resources, resulting in shifts in agro-climatic zones (Akhtar et al. 2008; Immerzeel et al. 2012; Adnan et al. 2022). Adnan et al. (2017) have specifically highlighted the vulnerability in the subbasin of UIB to these effects. Therefore, in order to plan and manage hydrological structures in Pakistan, it will be crucial to estimate water supplies in light of climate change.

The hydrological behavior of UIB in response to climatic change has been studied by using atmospheric input from different climate models (Naeem et al. 2012; Masood et al. 2020; Adnan et al. 2017; Latif et al. 2018; Hayat et al. 2019; Khan and Koch 2021). Global climate models (GCM) as a primary instrument are used extensively for analyzing future climate changes (Mishra et al. 2020). CMIP6 experiments by Eyring et al. (2016) and Marotzke et al. (2017) have been focused on identifying extreme climate changes in the future, past, and physical processes. Precipitation trend in various climatic zones of Pakistan over the recent decades was detected significant reduction in winter, summer, and annual precipitation (Salma et al. 2012). Waseem et al. (2021) and Cook et al. (2020) indicated that temperature remained to increase and precipitation declined from historical to the future and intensity of drought would increase in the near future based on projections of CMIP5 and CMIP6 data, respectively. Ensemble means of CMIP5 and CMIP6 models from the HighResMIP experiment were used to investigate atmospheric trends in Iran, under a high emission scenario and conclude that significant changes are expected for Iran as consequence of climate change and the anthropogenic influence (Usta et al. 2022a, b, c). Shafeeque and Luo (2021) proposed a multi-perspective approach and applied in UIB as a case study to select the best-suited set of GCMs for climate change assessments on glacio-hydrology. According to Atif et al. (2019), the UIB is likely responsible for more than 90% of the Indus River's low-land flow, while the sub-basins of the UIB, including Shyok, Shigar, Astore, Gilgit, and Hunza, are responsible for 60% of the Indus River's total annual discharge. Naeem et al. (2012) and Wang et al. (2017) suggested that with an increase in glacier cover, the management of runoff by glaciers has become increasingly important. Since Pakistan's economy and a sizeable portion of its population (about 207 million people) rely heavily on snow and glacier meltwater of UIB, it is imperative to assess how these water resources will adapt to IPCC climate change scenarios (Atif et al. 2019). The hydrological models to quantify the streamflow of glaciated subbasins of UIB had been explored by few studies (Akhtar et al. 2008; Tahir et al. 2011; Zhang et al. 2016; Adnan et al. 2017; Garee et al. 2017;Ali et al. 2018; Hayat et al. 2019). However, these studies did not take glacier melt into account because of the models limitations e.g. (Tahir et al. 2011; Adnan et al. 2017; Hayat et al. 2019). All three of these studies used Snowmelt Runoff Model (SRM) which is based on temperature index approach and does not take into account glacier melt to simulate the streamflows of Gilgit, Hunza and Astore subbasins, respectively. Garee et al. (2017) applied Soil and Water Assessment Tool (SWAT) model over Hunza River Basin using elevation band and snowmelt algorithm. Overall the results were satisfactory, however, runoff by glacier melt were not estimated due to incapability of SWAT dealing with glaciers which causes the uncertainty in hydrological balance of Hunza River Basin. Akhtar et al. (2008) predicted the future flows using only one GCM data. Furthermore, Ali et al. (2018) applied Hydrologiska Byrans Vattenbalansavdeling (HBV) model to predict the streamflow of Hunza River Basin under climate change scenarios by CMIP5. In the modified version of HBV model, the snow melt routine was altered slightly, and glacier ice melt and accumulation were represented. Astore River Basin is one of the crucial basins and is covered with snow most of the time in the year, however, there is lack of knowledge about how changing climate simulated by GCMs under scenarios by latest report of CMIP6 will effect water resources of a basin where significant portion of streamflow is from snow and glacier melts.

In order to fill the gap left by earlier researches, the current study uses University of British Colombia (UBC) Watershed Model (WM), the top-ranked medium complexity hydrologic model for mountainous watersheds in Alberta and British Columbia, to analyze the hydrological balance of the Astore River Basin in depth (Beckers et al. 2009). While, climate data of CMIP6 is used unlike other studies which used CMIP5 data. CMIP6 gives data of climate parameters (e.g. precipitation and temperature) under Shared Socio-economic Pathways (SSP). Shared Socio-economic Pathways (SSPs) were developed as an addition to Representative Concentrated Pathways (RCPs) to address the various socio-economic challenges that need adaptation and mitigation (O'Neill et al. 2014). The CMIP5 data set contains projections developed by using the Representative Concentration Pathways (RCPs), as well as time series of emissions and concentrations of all greenhouse gases (GHGs), aerosols, and chemically active gases, as well as land use and land cover (Moss et al. 2008). This study examines the potential acceleration of climate change and subsequent hydrological implications of the Astore river basin in the Upper Indus Basin (UIB), Pakistan, in light of climate change factors and updated climate forecasts.

In this study we provide an update on the impacts of future climate change on water resources of Astore river basin using UBC Watershed Model under different CMIP6 scenarios. Specifically the objectives of this study are (a) to analysis the spatial-temporal variation in climate variables using CMIP6 data and (b) to evaluate the climate change impacts on hydrological processes in Astore River Basin. Overall study findings will aid in comprehension of the high mountain hydrological process and be helpful in future strategic planning for water resources, management, and sustainability in the region.

2 Study Area

The Astore watershed (sub-basin of the UIB) located between 35°16´-35°45´ N and 74°70´-74°86´ E (Fig. 1), is selected for hydro-glaciological modeling under future climate change. The Astore River basin, which drains an area of roughly 3988 km², is situated in the northwest of the Himalayan range with elevation ranging from 1198 m to 8069 m. Glaciers span around 543 km² of land. The ninth highest mountain of the world- the Nanga Parbat also lies in the basin (Afshan et al. 2009). In winter, the major part of the basin remain covered with snow and glaciers which is 15% of the entire area (Naeem et al.

2012). The mean annual temperature in the valley Rattu (2718 m) was 9.9°C, and 2.9°C in Rama (3179 m) at a higher altitude from 1998 to 2012 (Farhan et al. 2015).

The two-thirds of precipitation in Astore basin are mainly due to westerly circulations in winter and spring, while remaining one third of precipitation in summer and autumn is forced by monsoon system. The snow cover in the basin remains ≈ 7% in summer and ≈ 95% in winter (Tahir et al. 2016). The Astore watershed is covered in a variety of land types, including vegetation, rivers, lakes, and glaciers. The majority of the vegetation consists of broad and needle mixed woods, coniferous and broadleaf forests, and grasslands are perennials and can withstand freezing temperatures

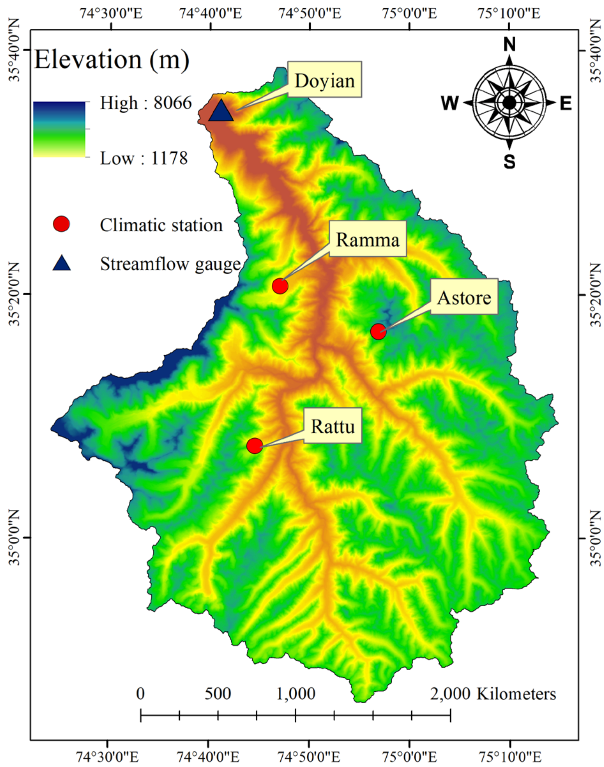

Fig. 1 Location of the Astore Basin with meteorological and hydrological stations.

3 Data and Methodology

3.1 Datasets

3.1.1 Hydro-meteorological data

Daily streamflow data of the Astore River at Doyian gauging station for the period 1990-2014 and meteorological data comprising maximum and minimum temperature, solar radiation and precipitation from two automatic weather stations (AWS) named as Rama and Rattu for the period 1995-2020 were received from Water and Power Development Authority (WAPDA), Pakistan (Table 1). However, the meteorological data of Astore station was obtained from the Pakistan Meteorological Department (PMD).

3.1.2 Spatial data

The digital elevation model (DEM) of 30 meter resolution by the Shuttle Radar Topography Mission (SRTM) of U.S. National Aeronautics and Space Administration (NASA) was obtained through its website (https://search.earthdata.nasa.gov/search). According to the criteria of the hydrological model, the study area was divided into seven elevation classes. Arc GIS was used to calculate the mean elevation of each class. Most of the area of Astore watershed that is about 1983 km² or 49.17% lies between elevations ranging from 3805 to 4616 m (Table 2). Glacier data was obtained from the Randolph Glacier Inventory 6.0 (https://www.glims.org/RGI/rgi60_dl.html). Land use data with spatial resolution of 900 meter was obtained from https://due.esrin.esa.int/page_globcover.php (Bontemps et al. 2011). Fig. 2 and Table 2 present the features of glacier areas and land-use statistics in different elevation zones.

3.2 Global climate model

The selection of Global Climate Models (GCMs) depends on whether they provide the necessary input variables for hydrological models. These input variables are precipitation, maximum temperature, and minimum temperature which are available for five different shared socioeconomic pathways (SSP1-

Table 1 Detail of hydro-meteorological stations with dataset's agencies in Astore River Basin

Station Name	Latitude (N)	Longitude (E)	Data	Agency	Elevation (m)
Astore	35.36°	74.86°	Climatic	PMD	2183
Rama	34.45°	74.77°	Climatic	GMRC-WAPDA	2718
Rattu	35.16°	74.78°	Climatic	GMRC-WAPDA	3179
Doyian	35.54°	74.70°	Hydrological	SWHP-WAPDA	1583

Table 2 Features containing inputs of the UBC watershed model

Bands	Elevation class (m)	Mean elevation (m a.s.l.)	Area (km²)	% of Total area	Glacier area (km²)	Total green area (km²)	Tree canopy index	Impermeable area (fraction)
1	1178-2725	1979	196	4.90	0	164.16	0.72	0.00
2	2725-3332	3031	474	11.89	2.28	387.81	0.71	0.00
3	3332-3805	3570	751	18.82	13.80	582.30	0.67	0.02
4	3805-4210	4012	965	24.19	32.52	629.82	0.54	0.03
5	4210-4616	4419	1018	25.52	68.84	509.22	0.43	0.06
6	4616-5381	4993	521	13.05	116.57	122.76	0.21	0.20
7	5381-8066	6667	67	1.69	28.90	0.99	0.01	0.38

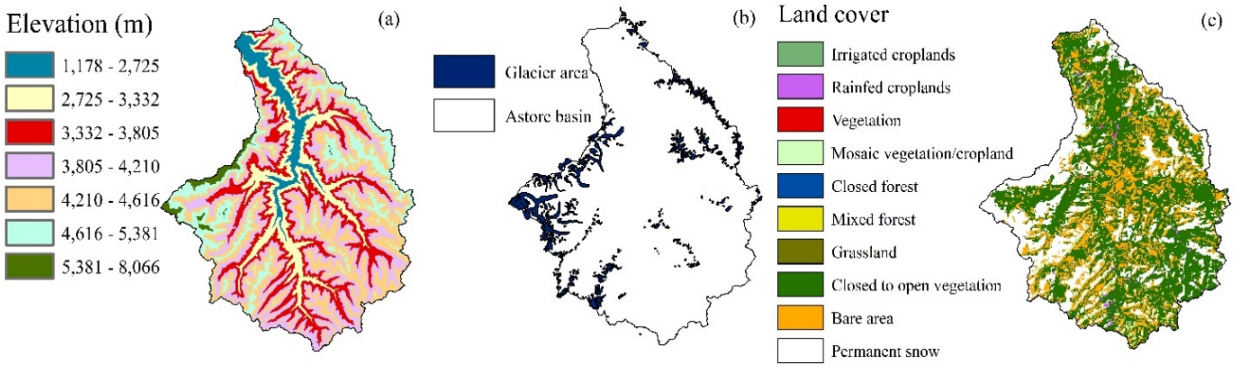

Fig. 2 Astore basin with elevation zones (a), glaciated area (b) and Land cover (c).

1.9, SSP1-2.6, SSP2-4.5, SSP3-7.0 and SSP5-8.5) from the Scenario Model Intercomparison Project (MIP). Different GCMs can have varying levels of accuracy and resolution so the selection of appropriate model is critical for reliable hydrological modeling. Numerous researchers analyzed precipitation, and maximum and minimum temperature using multiple GCM (more than one) because of computational limitations, resolution of data, availability of data against selected emission scenarios, and to compare different models performance (Ali et al. 2018; Syed et al. 2022; Waseem et al. 2021). For instance, the AWI-CM-1-1-MR model provides both maximum and minimum temperature data at a 100 km resolution, while CESM2, CESM-WACCM, CESM-WACCM-FV2, and CMCC-CM2-SR5 only provide precipitation data at the same resolution. EC-Earth3-AerChem includes all the necessary input variables for only one SSP scenario, and EC-Earth3-CC, HadGEM-GC31-MH and GFDL-CM4 are providing data for two SSP scenarios on a daily basis at a 100 km resolution. Additionally, some of GCMs such as FGOALS-3-H, GFDL-C4C192, and SAMO-UNION are not providing future projections of numerous meteorological inputs. Based on data required for hydrological model and high resolution of data i.e. 100 km, we chose the models named as BCC-CSM2-MR by Beijing Climate Center, China, INM-CM5-0 by Institute for Numerical Mathematics, Russian Academy of Science, Moscow, Russia and MPI-ESM1-2-HR by Max Planck Institute for Meteorology, Germany.

The SSPs reflect several potential land-use changes and greenhouse gas scenarios based on different hypotheses about economic development, global governance and climate mitigation efforts, as calculated using traditional valuation models (Kim et al. 2020; Kreienkamp et al. 2020). Based on these assumptions, the SSPs are used to produce various radiative forcing pathways and related warming up to the end of the 21st century (Meinshausen et al. 2020). The SSPs include socio-economic and environmental factors which make them more comprehensive than the previous Representative Concentration Pathways (RCPs). Additionally, the SSPs enable an integrated analysis of climate change mitigation, adaptation and sustainable development which is crucial for developing effective policy responses to global challenges. To look at a set of potential future contracts, we used a simulation of three SSPs obtained from Scenario MIP: SSP1-2.6 (+2.6 W/m²imbalance; low forcing sustainability pathway), SSP2-4.5 (+4.5W/m²; medium forcing middle-of-the-road pathway) and SSP5-8.5 (+8.5 W/m²; high-end forcing pathway). The diagnostic output of three climate models backed up with IPCC's sixth assessment report was obtained from the CMIP6 website (https://esgf-node.llnl.gov/).

3.3 UBC Watershed Model (WM)

UBCWM was developed by Quick and Pipes (1976) to simulate runoff from mountainous watersheds and has been continuously updated to its current form. The UBC model is a conceptual semi-distributed hydrological model which can simulate the runoff by snow and glacier melts and rainfall on hourly to daily basis and has been extensively used over the UIB basin (Adnan et al. 2022; Loukas and Vasiliades 2014; Naeem et al. 2015; Saeed et al. 2009). UBCWM was chosen as the hydrologic model of medium complexity with the highest ranking for mountainous watersheds of British Columbia and Alberta (Beckers et al. 2009). The UBCWM practices the hourly/daily point value data for precipitation, maximum and minimum temperatures to compute the streamflow. The inputs required are precipitation in millimeters and the temperature in degrees Celsius.

The UBCWM conceptualizes watershed as several elevation zones, since meteorological and hydrological processes in mountainous watersheds are functions of elevation (up to 12 elevation bands) (Quick and Pipes 1977). Being a key determinant of hydrologic behavior, the orographic gradients of precipitation and temperature in these watersheds are assumed to be identical for a precipitation event. These gradients are dealt by area-elevation band concept in the model. The model also offers details on watershed features like snow cover and snow water equivalent, evapotranspiration and interception losses, soil moisture, groundwater storage, and the surface and subsurface components of runoff for each elevation band, and for the whole watershed as well. The percent glacial coverage inside each elevation band, a model parameter, controls the amount of runoff from glaciers (Loukas and Vasiliades 2014).

For each elevation band, a collection of physiographic parameters such as mean band area, mean band elevation, impermeable area, forested areas, vegetation density, open areas, aspect, and glaciated area are used to describe the watershed and those can be estimated using maps and remotely sensed data (Naeem et al. 2012; Khan et al. 2014). Ten group of parameters make up an input file (.WAT file), and each one addresses a different part of the modelling process. These parameters provide a guidance to control the UBCWM-run (Shakir et al. 2010; Naeem et al. 2015). The flow chart (Fig. 3) displays the UBCWM's overall structure and adopted methodology.

3.4 Evaluation of future climate projections

Three GCMs namely BCC-CSM2-MR, INM-CM5-0, and MPI-ESM1-2-HR from Coupled Model Inter-comparison Project Phase 6 (CMIP6) were chosen for the precipitation and maximum and minimum temperature data. The dataset was downscaled by

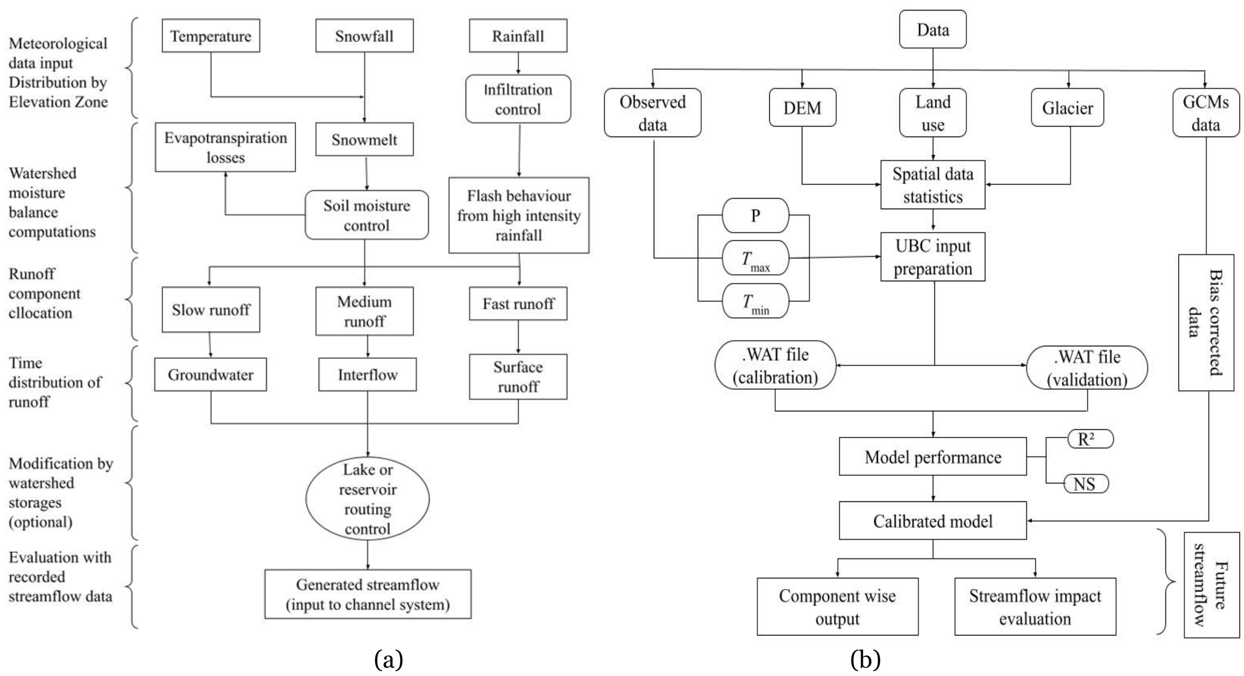

Fig. 3 Generalized flow chart of the UBC Watershed Model by Quick and Pipes (1977) (a), Schematic chart for this study using the UBCWM (b).

applying the Bias correction change factor approach. The evaluation was processed by determining the coefficient of determination (R^2) for a period 1995-2011 among the projections of historical data of selected GCMs and observational data and as listed in Table 3.

3.4.1 BIAS correction

The change factor (CF) method is a bias correction technique that reduces bias between observed or point data and model outputs (Chisanga et al. 2017; Berg et al. 2012; Shrestha et al. 2017). The method works by calculating a correction factor which further applies to adjust coarse scale data. Method like bias correction by statistical or dynamic downscaling has been used to make suitable the coarse scale GCM data for hydrological modelling and also bias correction method has been recommended and applied by numerous studies (Chiew et al. 2010; Fang et al. 2015; Pokhrel et al. 2020). Moreover, in the context of climate modeling, extrapolation refers to the process of estimating values of a variable outside the range of observed data. Extrapolation can lead to significant errors, particularly when there is limited data available to calibrate the model. The change factor method is designed to avoid extrapolation by using observed data to calibrate the model at the range of values that have been observed. Change factor method applies the monthly mean changes to the GCM output to adjust daily temperature and precipitation data series. The adjusted daily maximum and minimum temperatures ($T_{\max}$ and $T_{\min}$) were obtained by adding the monthly differences of reference and the future years. However, future precipitation was obtained by multiplying the ratio of future to the reference year's monthly series with the daily precipitation of the base year. The Eqs. (1), (2) for precipitation and temperature data are given below:

$$P_{\text{adj;fut;d}} = P_{\text{obs;d}} * \sum_{i=1}^{k} P_i \left(\frac{\bar{P}_{\text{GCM,futr m}}}{\bar{P}_{\text{GCM,ref m}}} \right) \quad (1)$$

$$T_{\text{adj;fut;d}} = T_{\text{obs;d}} + \sum_{i=1}^{k} P_i \left(\bar{T}_{\text{GCM,futr m}} - \bar{T}_{\text{GCM,ref m}} \right) \quad (2)$$

where, $P_{\text{adj;fut;d}}$ and $T_{\text{adj;fut;d}}$ are the future-adjusted daily precipitation and temperature series, respectively; $P_{\text{obs;d}}$ and $T_{\text{obs;d}}$ are observed daily precipitation and temperature; $P_{\text{GCM,futr}}$ m and $T_{\text{GCM,futr}}$ m *are* future mean monthly precipitation and temperature of climatic models, respectively; *and* $P_{\text{GCM,refr m}}$ *and* $T_{\text{GCM,refr m}}$ are base period mean monthly precipitation and temperature of climatic models, respectively. P_i is the grid weight of each GCM grid cell, and k is the total number of cells.

3.4.2 Trend analysis

In this study, trend analysis was performed to determine whether there are statistically significant trends and patterns over the basin or not. The analysis was carried out at Astore, Rama and Rattu stations using future data of selected climatic models (BCC-CSM2-MR, INM-CM5-0, and MPI-ESM1-2-HR) for the period 2020-2070. Mann Kendall (Mann 1945; Kendall 1975) technique was used for analyzing trend. The Mann Kendall test and Theil-Sen (Sen 1968) estimator have been recognized as well-known tools for detecting the trend and measuring the slope in meteorological and hydrologic time series (Shifteh Some'e et al. 2012; Iqbal et al. 2018; Atif et al. 2019). These methods have advantages in comparison to linear regression that the data do not require to be followed by a particular distribution and also handle the missing values. The equations for determining the MK test statistic S and the standardized test statistic Z are as follows:

$$S = \sum_{k=1}^{n-1} \sum_{j=k+1}^{n} sign(x_j - x_k) \quad (3)$$

$$sign(x_j - x_k) = \begin{Bmatrix} 1 \ if \ x_j - x_k > 1 \\ 0 \ \ if \ x_j - x_k = 1 \\ -1 \ if \ x_j - x_k < 1 \end{Bmatrix} \quad (4)$$

$$Var(S) = 1/18[n(n-1)(2n+5) - \sum_{p=1}^{q} t_p(t_p - 1)(2t_p + 5)] \quad (5)$$

Table 3 Features of three selected General Circulation Models (GCMs)

Institution ID	Modeling center	Model name	Historical Data	SSP Data
BCC	Beijing Climate Center, China Meteorological Administration, China	BCC-CSM2-MR	P, $T_{\max}$ & $T_{\min}$	SSP1-2.6, SSP2-4.5, SSP5-8.5
INM	Institute for Numerical Mathematics, Russian Academy of Science, Moscow 119991, Russia	INM-CM5-0		
MPI-M, DWD, DKRZ	Max Planck Institute for Meteorology, Deutscher Wetterdienst, Deutsches Klimarechenzentrum, Germany	MPI-ESM1-2-HR		

$$Z = \begin{bmatrix} \frac{S-1}{\sqrt{Var(S)}} & if\ S > 0 \\ 0 & if\ S = 0 \\ \frac{S+1}{\sqrt{Var(S)}} & if\ S < 0 \end{bmatrix} \tag{6}$$

Z values can be positive or negative, where positive values indicate an upward trend (i.e., rising) and negative values indicating a downward trend (i.e., declining) (Alhaji et al. 2018). For details of the no tations that used in these equations, Gocic and Trajkovic (2013) and Shadmani et al. (2012) are referred. A MAKESENS programme developed by Salmi et al. (2002) was used to perform the above-mentioned non-parametric tests.

The following Sen's estimate is made for the slope of trend over two observations from sample of N data across time interval j and k:

$$Q_i = \frac{x_{j-}x_k}{j-k} \quad for \quad j > k \tag{7}$$

The median of the N pairs of Q_i is Sen's estimate. N values can be ranked in the method from smallest to largest, and the Sen's slope is as follows:

$$Q_{\text{med}} = \begin{Bmatrix} Q_{\left[\frac{(N+1)}{2}\right]} & \text{if } N \text{ was odd} \\ \frac{1}{2}\left(Q_{\frac{N}{2}} + Q_{[(N+2)/2)]}\right) & \text{if } N \text{ was even} \end{Bmatrix} \tag{8}$$

3.4.3 Prediction of future streamflow under climate change scenarios

The calibrated UBCWM was used to project the future streamflow for the period 2020–2070 in the Astore River Basin by forcing the bias corrected projected data from three GCMs under three scenarios namely SSP1-2.6, SSP2-4.5, and SSP5-8.5. To analyze the future climate change impact on streamflows, the future streamflow was compared with the period of 1990-2014. The relative changes in streamflow was evaluated by the following equation:

$$\delta R = \frac{\bar{R}_{(2020-2070)} - \bar{R}_{(1990-2014)}}{\bar{R}_{(1990-2014)}} \tag{9}$$

3.5 Model setup and evaluation

Since the UBCWM use the concept of area elevation band to cater the orographic effect, the area was divided in seven elevation band. The meteorological inputs and the .WAT file (description of watershed) was prepared as per highlights of UBCWM manual. The most of the parameters has already been tested against quality data around the globe including British Columbia catchments and the Himalayas, and their default values require not to be altered (Quick et al. 1995). Moreover, in order to manage flow in mountainous catchment a subset of important parameters of UBCWM has been studied (Naeem et al. 2015). Accordingly, the characteristics of area and parameters that are used for Astore basin are summarized in Tables 2 and 4. The parameters POSREPO, PORREPO, POGRADL, EOLMID, POGLTK, and POISTK are related to climate, whereas COIMPA, POPERC, PODZSH, CORIEN, POALBMIN, AOEDDF, PABASE, POVBMX, and PODZTK are related to the physiographical characteristics of a watershed.

The UBCWM was calibrated and validated at daily timescales for the periods 2000-2004 and 2005-2009, respectively, with observed streamflows at Doyian hydrological station in Astore basin (Fig. 4). The model performance was evaluated using the two statistical indicators coefficient of determination (R^2) and the Nash–Sutcliffe coefficient (NS), as suggested by (Moriasi et al. 2007). Their respective equations are as follows:

$$R^2 = \left[\frac{\sum_{i=1}^{n}(Q_o - \bar{Q}_o)(Q_s - \bar{Q}_s)}{\sqrt{\sum_{i=1}^{n}(Q_o - \bar{Q}_o)^2 \sum_{i=1}^{n}(Q_s - \bar{Q}_s)^2}}\right]^2 \tag{10}$$

$$\text{NS} = 1 - \frac{\sum_{i=1}^{n}(Q_0 - Q_s)^2}{\sum_{i=1}^{n}(Q_0 - \bar{Q}_o)^2} \tag{11}$$

where, n denotes the number of data points; Q_s and Q_o are the simulated and observed runoff at ith time step; $\bar{Q}_s$ and $\bar{Q}_o$ denote the simulated and observed runoff, respectively.

The R^2 and NS values at daily timescale were 0.82 during calibration period and 0.84 and 0.83 respectively, for the validation period. Simulated and observed streamflows are presented in Fig. 4. The overall satisfactory results lead the applicability of calibrated model to simulate the future flows for determining the hydrological response by forcing the selected GCMs data.

4 Results and Discussion

The GCMs data from three modeling centers Beijing Climate Center, China (BCC-CSM2-MR), Institute for Numerical Mathematics, Russia (INM-CM5-0), and Max Planck Institute for Meteorology Germany (MPI-ESM1-2-HR) presented well-established correlations with observed data of precipitation (P), maximum temperature (T_{max}) and minimum temperature (T_{min}), and forced into hydrological model (the UBCWM) for projecting the hydrological response in Astore basin.

Coefficient of determination (R^2) among climate model's historical projections (T_{max}, T_{min} and P) and observational data for the year 1995-2011 are shown in Figs. 5, 6 and 7. MPI-ESM1-2-HR exhibited better results that ranged from 0.70 to 0.74 for precipitation and 0.90-0.92 for T_{max} and T_{min} at Astore, Rama, and Rattu stations followed by INM-CM5-0 and BCC-CSM2-MR where (R^2) ranged between 0.59-0.69 for P and 0.74-0.92 for T_{max} and T_{min}.

4.1 Projection of precipitation under SSPs scenarios

Describing the complicated terrain of the Astore River basin, there are significant uncertainty in the expected precipitation statistics under several scenarios (Khan and Koch 2021). In accordance with Almazroui et al. (2021), the trend analysis results of this study (Table 5) also show that the variation in precipitation magnitude under all SSPs scenarios is not constant with respect to GCMs and seasons during the studied period. In order to conduct spatial and temporal analysis, future projections of precipitation and temperatures for the time period of 2020-2070 were analyzed at annual and seasonal timescales (winter-DJF, spring-MAM, summer-JJA and autumn-SON).

The annual precipitation under SSP1-2.6 and SSP5-8.5 by BCC-CSM2-MR showed insignificant decreasing trend with a magnitude of 7.64 mm/decade and significant decreasing trend of 22.62 mm/decade at 90% confidence interval, respectively. Conversely, MPI-ESM1-2-HR and INM-CM5-0 showed a significant increase ranging from 18.72 to

Table 4 Best-suited calibrated parameters of the UBCWM for Astore basin

No.	Parameters	Description	Range	Best suited value
1	POSREPO	Adjustment to precipitation when average temperature < 0 (snowfall)	-1.0–1.0	0
2	PORREPO	Adjustment to precipitation when average temperature > AOFORM (rain)	1.0 – 1.0	0
3	POGRADL	Precipitation gradient factor (%) for elevations below EOLMID	0 - 20	15
4	ELOMID	Elevation at which POGRADM is effective (m)	-	4000
5	COIMPA 7 elevation bands of the watershed	Fraction of impermeable area in the band	- -	0, 0, 0.02, 0.03 0.06, 0.20, 0.38
6	POPERC	Groundwater precipitation in mm/day	-	95
7	PODZSH	Deep zone share fraction	0 – 1.0	0.12
8	POALBMIN	Albedo of very aged snowpack	-	0.3
9	AOEDDF	Potential evapotranspiration factor in mm/day	0-0.5	0.03
10	PABASE	The albedo initial decay value	-	0.4
11	POVBMX	Maximum wind speed (km/h)	-	12
12	PODZTK	Time constant for deep groundwater runoff (days)	100-300	300
13	A0PPTP	Threshold precipitation for temperature lapse rate (mm)	-	5
14	A0TLZP	Temperature lapse rate (°C /1000 m) when precipitation > A0PPTP	-	6.5

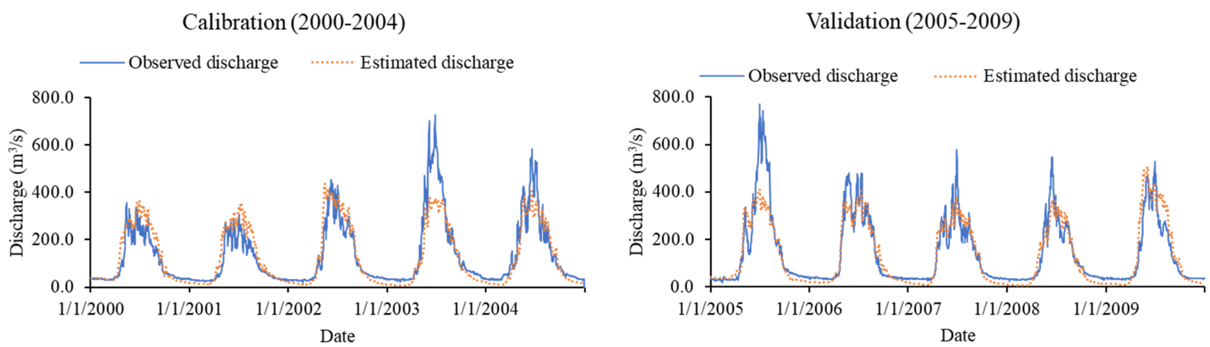

Fig. 4 Hydrograph between observed and estimated streamflows from UBCWM during calibration period: 2000-2004 and validation period: 2005-2009.

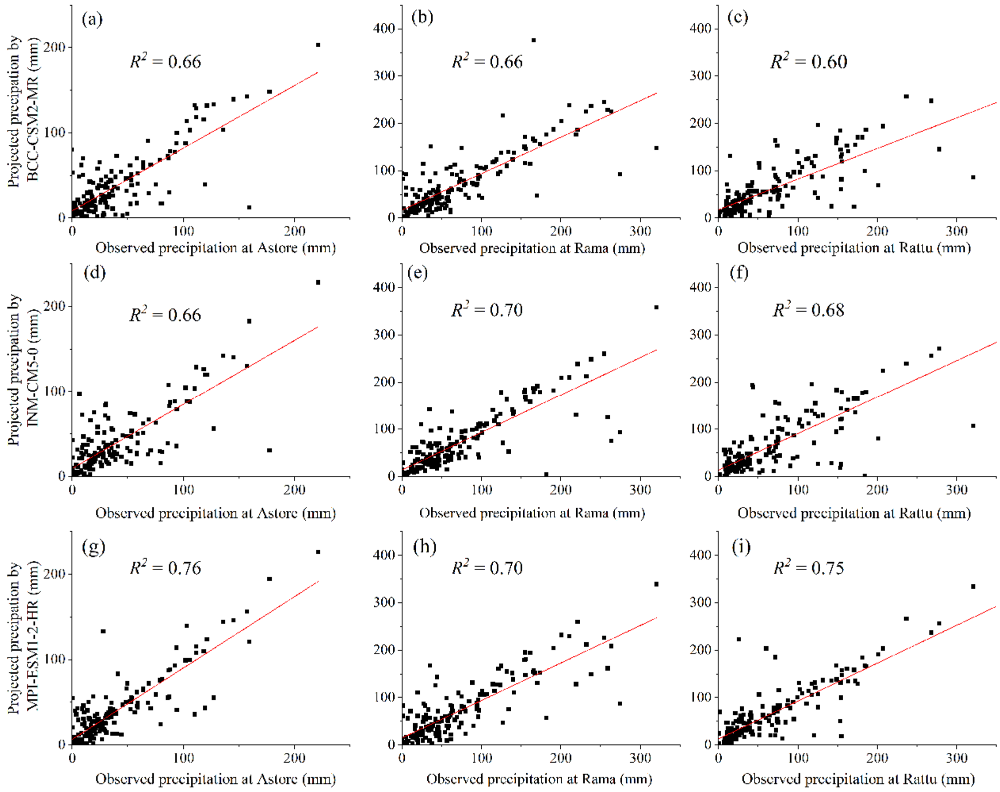

Fig. 5 Coefficient of determination (R^2) between observed daily precipitation and GCM (a-c) BCC-CSM2-MR, (d-f) INM CM5-0 and (g-i) MPI-ESM1-2-HR during the period of 1995-2011.

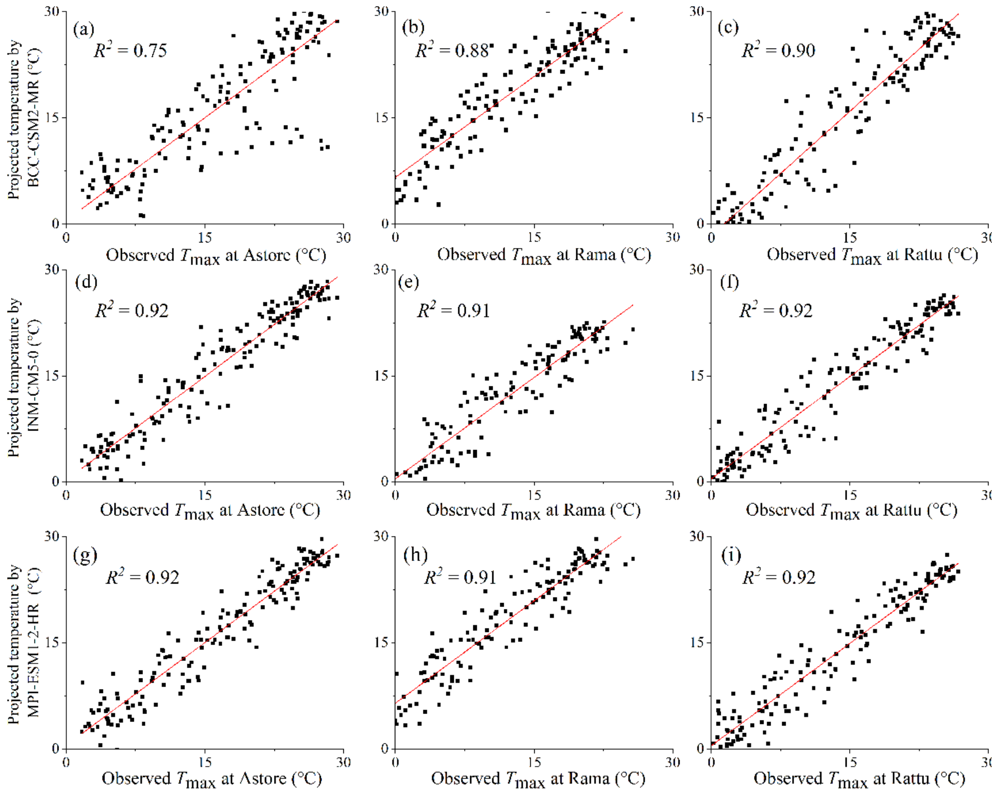

Fig. 6 Coefficient of Determination (R^2) between observed daily maximum temperature and GCM (a-c) BCC-CSM2-MR, (d-f) INM-CM5-0 and (g-i) MPI-ESM1-2-HR during the period of 1995-2011.

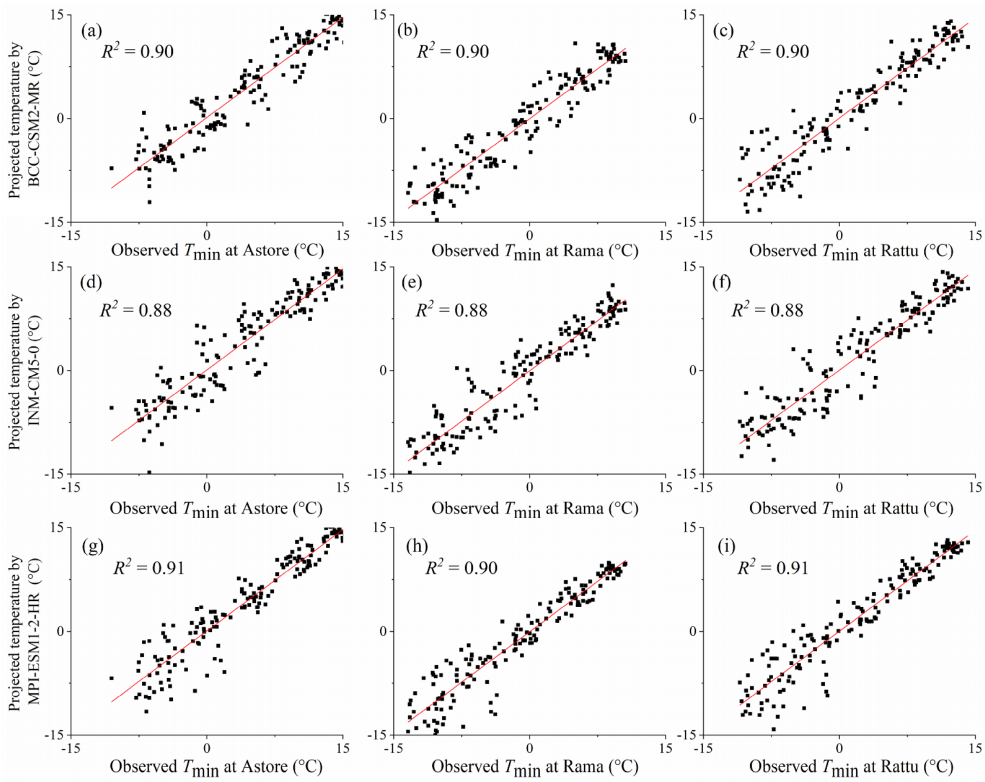

Fig. 7 Coefficient of Determination (R^2) between observed daily minimum temperature and GCM (a-c) BCC-CSM2-MR, (d-f) INM-CM5-0 and (g-i) MPI-ESM1-2-HR during the period of 1995-2011.

Table 5 Change in magnitude of annual and seasonal precipitation (mm decade^{-1}) of Astore basin

Period	GCMs		Winter (DJF)	Spring (MAM)	Summer (JJA)	Autumn (SON)	Annual (J-D)
2020-2070	SSP1-2.6	BCC-CSM2-MR	4.75	1.70	-10.18***	3.26	-7.64
		MPI-ESM1-2-HR	12.30	8.10	-4.39	2.43	26.55+
		INM-CM5-0	3.29	-5.84	1.93	15.94**	18.72+
	SSP2-4.5	BCC-CSM2-MR	7.48	4.91	-7.98	3.83	3.41
		MPI-ESM1-2-HR	12.62	-1.48	2.11	-4.28	6.91
		INM-CM5-0	0.56	-7.69	4.36	-0.31	1.26
	SSP5-8.5	BCC-CSM2-MR	-3.61	-10.93	1.08	-2.61	-21.62+
		MPI-ESM1-2-HR	15.18+	-8.50	0.63	6.36	19.99
		INM-CM5-0	-9.40	-6.60	2.31	17.21	7.94

Note: *** shows trend is significant at 99.99% confidence level, ** shows trend is significant at 99% confidence level, * sign shows trend is significant at 95% confidence level and "+" sign show that trend is significant at 90% confidence level. In case of no sign it means trend is not significant at any significance level.

26.55 mm/decade under SSP1-2.6; a small range of change from 1.26 to 6.91 mm/decade under SSP2-4.5; and from 7.94-19.99 mm/decade under SSP5-8.5 as presented in Fig. 8 and Table 5. Similar increasing trend of mean precipitation was found by Atif et al. (2019) at Astore Basin under the RCP8.5 and RCP4.5 scenarios.

The seasonal precipitation analysis showed a decreasing trend in summer under SSP1-2.6 and SSP2-4.5 of BCC-CSM2-MR and MPI-ESM1-2-HR. However, precipitation in winter, spring, and autumn seasons presented increasing trend. Specifically, in autumn INM-CM5-0 showed a significant increasing trend at 95% of the confidence interval with a magnitude of 15.95 mm decade-1 and insignificant decreasing trend was found in spring (Table 5). SSP2-4.5 scenario by all selected climate models displayed an increase in winter precipitation ranging from 0.56-12.62 mm decade-1, and a similar increasing trend was observed during the summer season. For spring

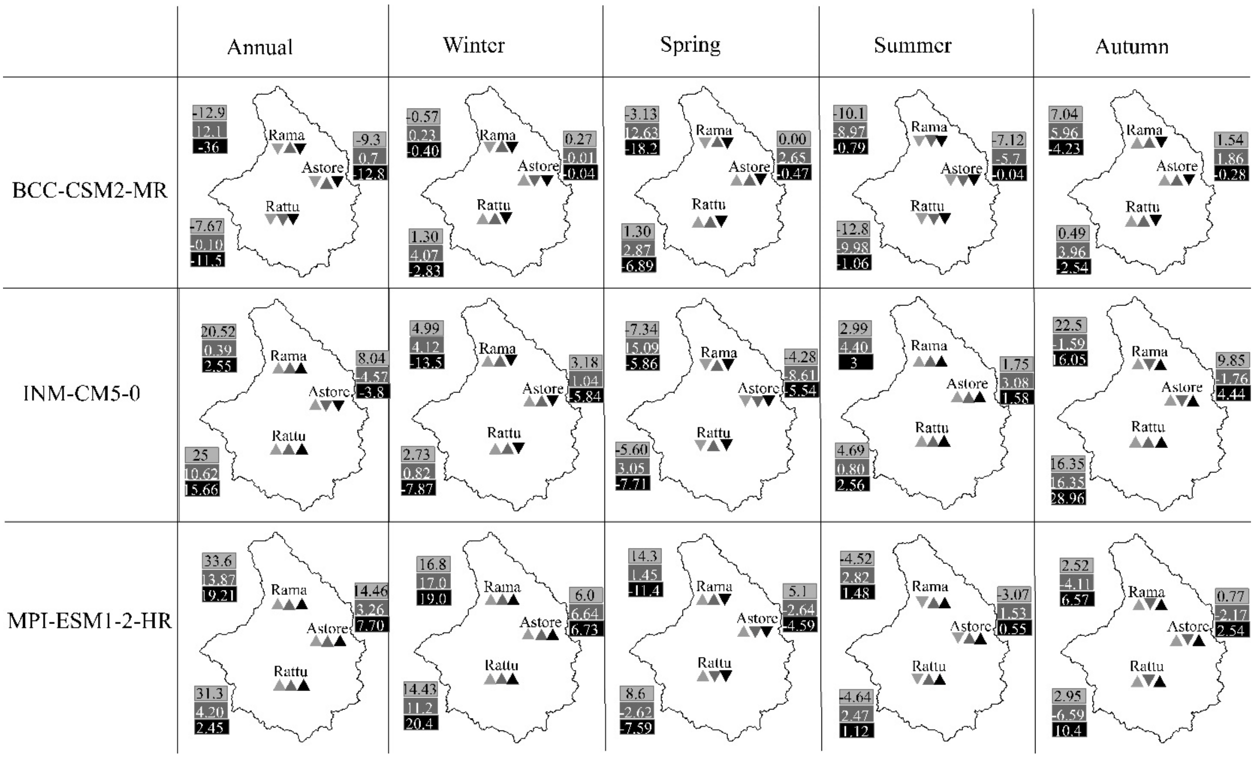

Fig. 8 Change in precipitation (mm/decade) under SSP1-2.6 (grey), SSP2-4.5 (dark grey) and SSP5-8.5 (black) scenarios at Astore, Rama and Rattu meteorological stations.

Table 6 Change in magnitude of annual and seasonal maximum temperature (°C/decade) of Astore basin

Period		GCMs	Winter (DJF)	Spring (MAM)	Summer (JJA)	Autumn (SON)	Annual (J-D)
2020-2070	SSP1-2.6	BCC-CSM2-MR	0.11+	0.06	0.43*	0.20	0.19**
		MPI-ESM1-2-HR	-0.07	-0.11	0.18***	0.06	0.02
		INM-CM5-0	0.49*	0.39*	-0.31*	-0.66*	0.00
	SSP2-4.5	BCC-CSM2-MR	0.30**	0.87*	0.58*	0.25**	0.44*
		MPI-ESM1-2-HR	0.40*	0.27	0.29*	0.21+	0.31*
		INM-CM5-0	0.65**	0.61*	-0.14***	-0.14	0.29*
	SSP5-8.5	BCC-CSM2-MR	0.67*	0.85*	0.84*	0.63*	0.84*
		MPI-ESM1-2-HR	0.26+	1.12**	0.54*	0.53*	0.49*
		INM-CM5-0	1.11*	0.73*	0.05	0.21	0.53*

(**Notes:** *** shows that trend is significant at 99.99% confidence level, ** shows that trend is significant at 99% confidence level, * sign shows that trend is significant at 95% confidence level and "+" sign shows that trend is significant at 90% confidence level. In case of no sign it means trend is not significant at any significance level).

and autumn, BCC-CSM2-MR showed an increasing trend while MPI-ESM1-2-HR and INM-CM5-0 exhibited a decrease in precipitation under SSP2-4.5.

Moreover, all climate models demonstrated a decreasing trend in spring and an increasing trend in summer under SSP5-8.5. BCC-CSM2-MR showed a decrease in precipitation during winter and autumn, while an increase in precipitation was presented by MPI-ESM1-2-HR during the same seasons. INM-CM5-0 exhibited a decreasing trend with a magnitude of 9.40 mm decade-1 in winter and an increasing trend of 17.21 mm decade-1 in spring under SSP5-8.5. These results were consistent with the findings of Ikram et al. (2016). Overall, in the Astore basin, all selected climate models displayed an increasing trend in summer and a decreasing trend in spring and autumn under both SSP2-4.5 and SSP5-8.5 scenarios

4.2 Projection of maximum temperature under SSPs scenarios

Table 6 and Fig. 9 presented annual and seasonal changes in T_{max} for the period 2020-2070. The analysis revealed that annual maximum temperature

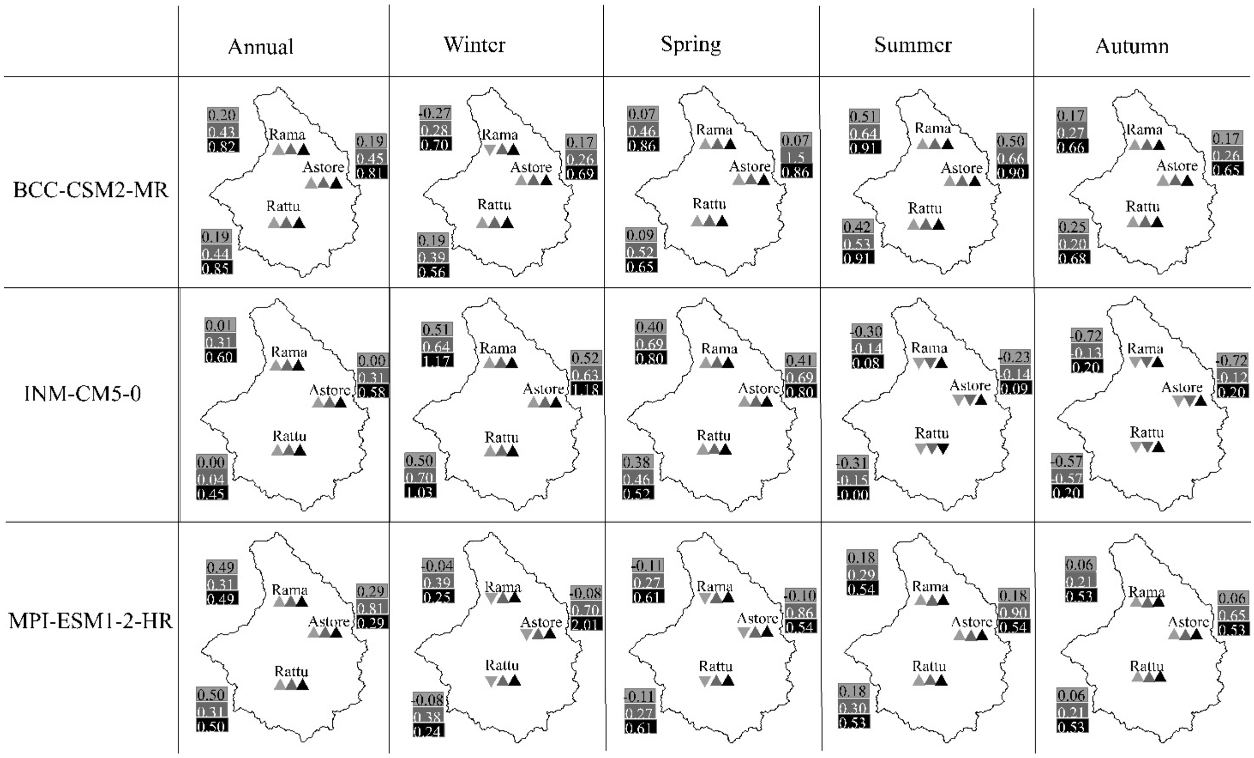

Fig. 9 Change in maximum temperature (°C/decade) under SSP1-2.6 (grey), SSP2-4.5 (dark grey) and SSP5-8.5 (black) scenarios at Astore, Rama and Rattu meteorological stations.

exhibited minimal change under SSP1-2.6 by all selected climate models. Annually under SSP2-4.5, temperature is predicted to increase by 0.29 - 0.44°C/decade at 95% confidence level. Additionally, there was a significant increasing trend under SSP5-8.5 with a magnitude ranging from 0.49 to 0.84°C /decade.

Seasonally, BCC-CSM2-MR under SSP1-2.6 demonstrated an upward trend with the magnitude of 0.11°C/decade, 0.06°C/decade, 0.43°C/decade, and 0.20°C/decade during winter, spring, summer, and autumn, respectively. On the other hand, INM-CM5-0 predicted a decreasing trend of 0.66°C/decade during summer and autumn, and an increase in temperature during winter and spring with rates up to 0.49°C/decade. MPI-ESM1-2-HR demonstrated a cooling trend in winter and spring with the rate up to 0.11°C/decade, and warming trend with magnitude up to 0.18°C/decade in autumn and summer. Overall, G CMs showed an increasing trend during all seasons except during summer and autumn where INM-CM5-0 exhibited an insignificant decreasing trend with a rate of 0.14°C/decade.

Moreover, BCC-CSM2-MR showed a warm spring with a rate of 0.87°C/decade under SSP2-4.5. BCC-CSM2-MR exhibited warm temperatures with the rate of change ranging from 0.63 to 0.85°C/decade during all seasons under where spring showed maximum rate and minimum rate occurred in autumn. MPI-ESM1-2-HR under SSP5-8.5 during winter, spring, summer, and autumn were the hottest with rate of change of 0.26, 1.12, 0.53, and 0.54°C/decade, respectively. Similarly, INM-CM5-0 also demonstrated a significant increase in temperature during winter and spring with the rate of 1.11 and 0.73°C/decade, respectively.

SSP5-8.5 represents a severe climate change scenario associated with high-end forcing pathways resulting from the increased emission of greenhouse gases and population growth. Consequently, there will be a greater rise in temperature under SSP5-8.5 as compared to other scenarios. According to Arfan et al. (2019), Astore, Gupis, Gilgit, and Skardu meteorological stations have shown the strongest warming trend with a temperature rise of 0.49°C /decade at 99.9% significance level. Additionally, annual and seasonal temperature changes differ across each subbasin due to various catchment features as highlighted by Iqbal et al. (2018).

Table 7 Change in magnitude of annual and seasonal minimum temperature (°C/decade) of Astore basin

Period		GCMs	Winter (DJF)	Spring (MAM)	Summer (JJA)	Autumn (SON)	Annual (J-D)
2020-2070	SSP1-2.6	BCC-CSM2-MR	0.16+	0.02	0.14+	0.10	0.08
		MPI-ESM1-2-HR	-0.23	-0.09	0.12**	0.06	0.00
		INM-CM5-0	0.43+	0.07	-0.25***	-0.09	-0.02
	SSP2-4.5	BCC-CSM2-MR	0.36**	0.82+	0.21**	0.32*	0.35*
		MPI-ESM1-2-HR	0.59**	0.19	0.29*	0.23+	0.34*
		INM-CM5-0	0.76*	0.34*	-0.07	-0.08	0.26*
	SSP5-8.5	BCC-CSM2-MR	0.84*	0.72*	0.57*	0.42*	0.64*
		MPI-ESM1-2-HR	0.23	0.94*	0.55*	0.56*	0.50*
		INM-CM5-0	1.16*	0.50*	0.12+	0.39***	0.51*

(**Note:** *** shows trend is significant at 99.99% confidence level, ** shows trend is significant at 99% confidence level, * sign shows trend is significant at 95% confidence level and "+" sign show that trend is significant at 90% confidence level. In case of no sign it means trend is not significant at any significance level).

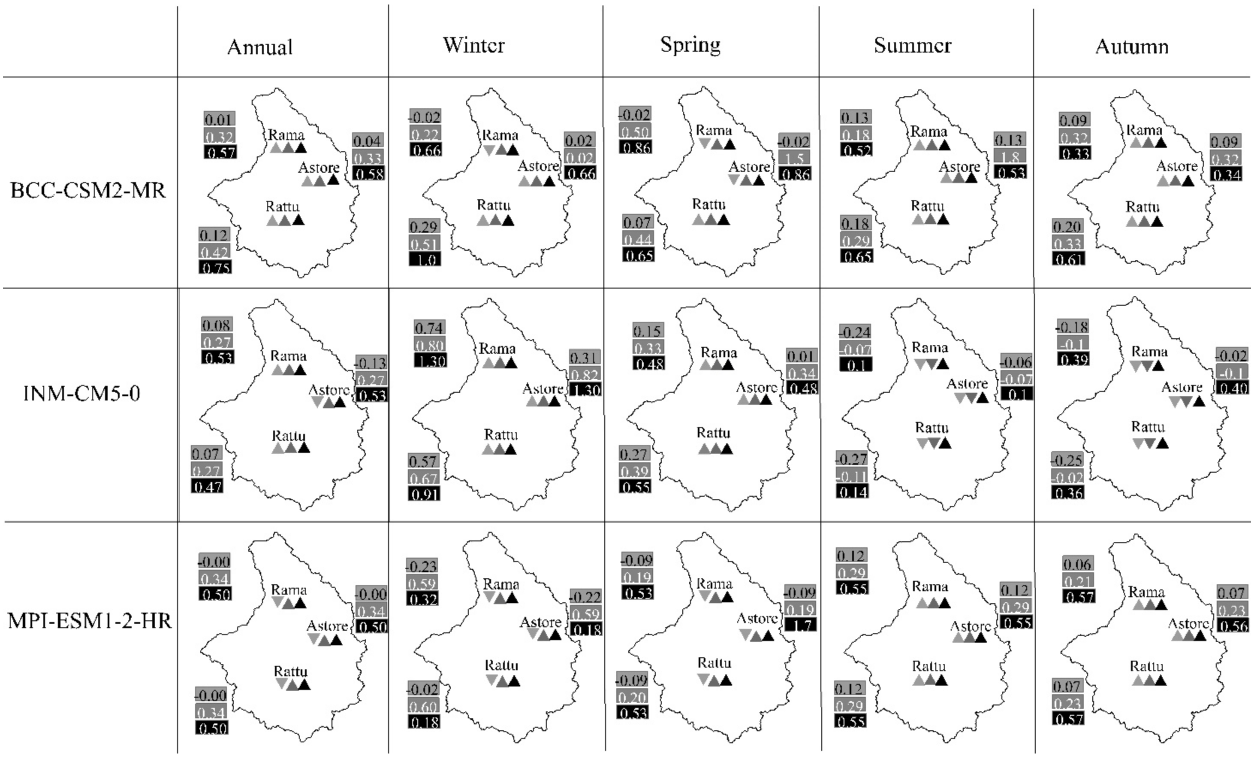

Fig. 10 Change in minimum temperature (°C/decade) under SSP1-2.6 (grey), SSP2-4.5 (dark grey) and SSP5-8.5 (black) scenarios at Astore, Rama and Rattu meteorological stations.

4.3 Projection of minimum temperature under SSPs scenarios

Table 7 and Fig. 10 depicted the annual and seasonal changes in T_{min} for the period 2020-2070. According to the analysis, BCC-CSM2-MR predicted a slight increase; INM-CM5-0 predicted a decrease; and MPI-ESM1-2-HR predicted no change in the average annual T_{min} under SSP1-2.6. However, under SSP2-4.5 and SSP5-8.5, GCMs demonstrated significant increase ranging from 0.26-0.35 and 0.51-0.64 °C/decade, respectively by the end of the 2070s.

BCC-CSM2-MR and MPI-ESM1-2-HR showed a significantly increasing trend with 90% significance level except MPI-ESM1-2-HR, which indicated a decreasing trend with magnitude of 0.23°C/decade whereas, under SSP2-4.5 and SSP5-8.5 respectively, all GCMs revealed a significant increase in minimum temperature with maximum magnitude of 0.76 and 1.16°C/decade by INM-CM5-0 climate model.

There was no change in minimum temperature during the spring under SSP1-2.6, while, a slightly significant increasing trends were observed under SSP2-4.5 and SSP5-8.5. Summer season under SSP1-

2.6 expressed a slightly increasing trend by all GCMs except INM-CM5-0 which showed a significant decreasing trend at 99.99% significance level with the magnitude of 0.25°C/decade (Table 7). BCC-CSM2-MR and MPI-ESM1-2-HR scenarios SSP2-4.5 and SSP5-8.5 showed an increasing trend with a magnitude up to 0.29 and 0.57°C/decade respectively, while INM-CM5-0 for same scenarios showed a slightly decreasing and increasing trend, respectively. During autumn, all GCMs showed almost no change under SSP1-2.6 while a slight change occurred under scenarios SSP2-4.5. However, a significant change increasing up to 0.56°C/decade occurred in autumn by SSP5-8.5 (Fig. 10).

4.4 Projection of streamflow under SSPs scenarios

Complicated hydrological processes and complex topography in mountainous watersheds, streamflow modelling is particularly difficult. According to discharge data from the last 25 years (1990-2014), the mean annual flow at Doyian hydrological station is 149.36 m³/s. The ability of hydrological models to replicate streamflow is often constrained by rates of change in temperature and precipitation with respect to elevation (Sleziak et al. 2021).

Fig. 11 presented the future streamflows simulated by the UBCWM model using projected climate data from three climate models (BCC-CSM2-MR, INM-CM5-0, and MPI-ESM1-2-HR) under three SSPs scenarios, namely SSP1-2.6, SSP2-4.5, and SSP5-8.5. Simulated streamflows for the period (2020-2070) projected to increase by all climate models under all scenarios except climate model BCC-CSM2-MR under SSP2-2.6 scenario which showed a slight decrease in streamflow. Overall, MPI-ESM1-2-HR projected the higher increasing rate of streamflows followed by BCC-CSM2-MR and INM-CM5-0. This increase may attribute to increase in precipitation and increase of glacier melts and also in accordance with Baig et al. (2021).

4.5 Contribution on runoff

The contributions to runoff from rainfall, snowmelt, ground water and glacier melt were

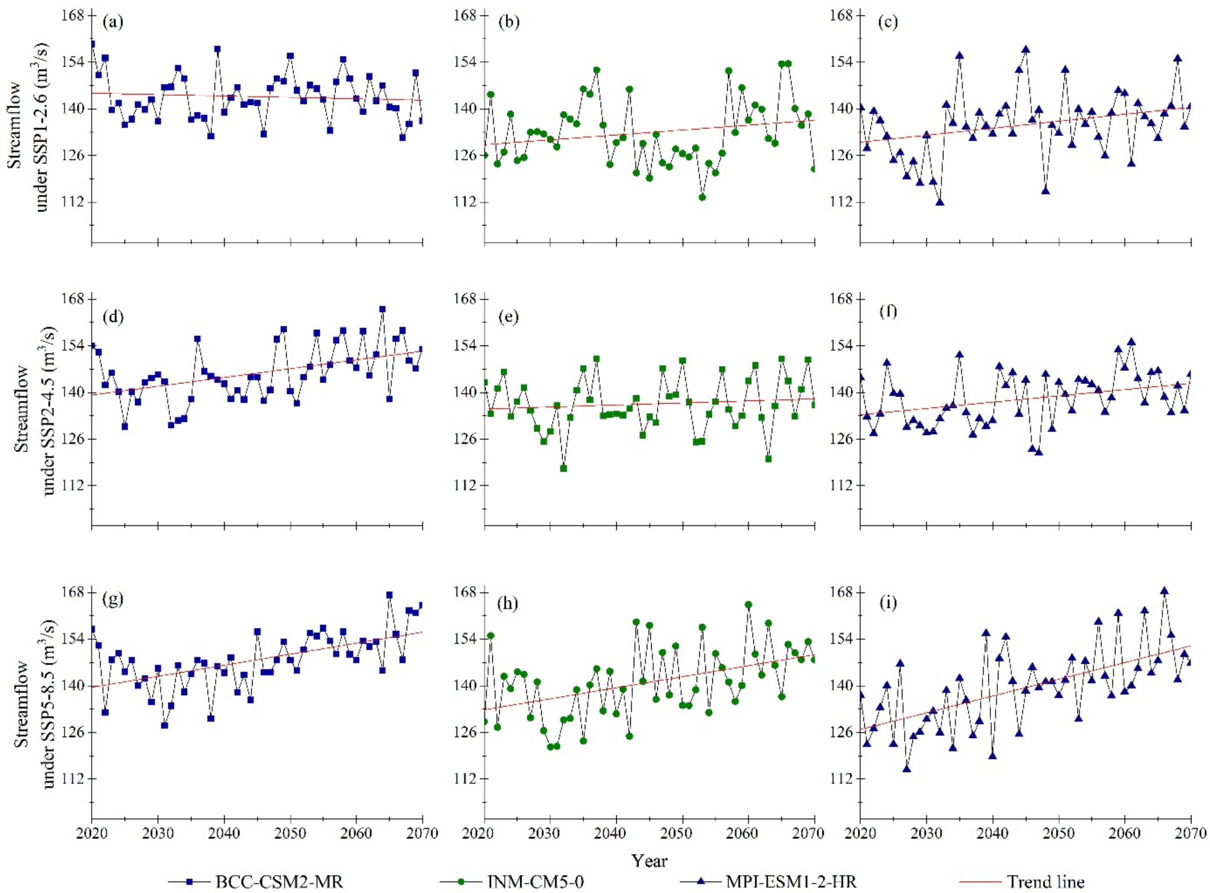

Fig. 11 Projected streamflows for the period 2020-2070 under SSP1-2.6 (a-c), SSP2-4.5 (d-f) and SSP5-8.5 (g-i) scenarios.

extracted from outputs of the UBCWM. Temperature influences both the melting of glaciers and the snowpack (Hassan et al. 2017). The change of precipitation and temperature can effectively explain the features of streamflow event in basin located in cold climate (Wang et al. 2017).

All GCMs showed a greater contribution of glacier and rainfall outflow, while a less contribution by snowmelt and groundwater at SSP1-2.6, SSP2-4.5, and SSP5-8.5, as shown in Fig. 12. In the Karakoram region, snowmelt contributes a major portion to the streamflow followed by glacier melt and rainfall (Ayub et al. 2020). These effects may because of adjusted parameters in the UBCWM.

The results presented more glacier contribution to streamflow under all scenarios ranging from 56-63.64%, followed by ground water, snowmelt and rainfall during the period of 2020-2070. The maximum contribution of glaciers and groundwater under SSP2-4.5 for BCC-CSM2-MR, INM-CM5-0 and MPI-ESM1-2-HR increased by 33.27%-61.72%, 33.79%-60.75% and 36.96%-56.81%, respectively. In comparison, rainfall and snowmelt show less than a 6% contribution to streamflow annually. Overall, all GCMs under all scenarios presented a similar behavior of contribution to runoff with maximum of glaciers and minimum by rainfall. However, more groundwater contribution than snowmelt may because of adjusted parameter in the model.

4.6 Impacts on future streamflows

For evaluating the influence to streamflow, the observed annual average flow (149.36 m^3/s) for the period of 1990 to 2014 was compared with the future simulated streamflows by climate model under three scenarios. Results showed by Table 8 are almost identical to those found by Hayat et al. (2019) where simulations were obtained by Snowmelt Runoff model (SRM) under RCP 2.6, 4.5, and 8.5 for the mid-21st century which showed that the mean river flow in the Astore basin increased by 13% to 29% in comparison to the base-year mean flow (128 m^3/s).

Results of all climate models showed a decrease in streamflow as compared to the period 1990-2014 with maximum change under SSP1-2.6 followed by SSP2-4.5 and SSP5-8.5 (Table 8). In context of future impacts INM-CM5-0 showed 11% decrease in streamflow of Astore River due to significant decrease in maximum and minimum temperature ranging from 0.09 to 0.66°C/decade in summer and autumn, respectively followed by MPI-ESM1-2-HR and BCC-CSM2-MR under scenarios SSP1-2.6. Similarly under scenario SSP2-4.5, all climate models showed a decrease in streamflow (2% to 9%) due to decreasing precipitation in spring, summer and autumn up to 10 mm/decade with a slight increase in temperature. Moreover, all climate models under scenario SSP5-8.5 showed a slight change towards decrease in future streamflow due to significant decrease of precipitation in all season and increase in temperature particularly in winter. The largest change was observed under SSP1-2.6, while a smallest one was presented by SSP5-8.5.

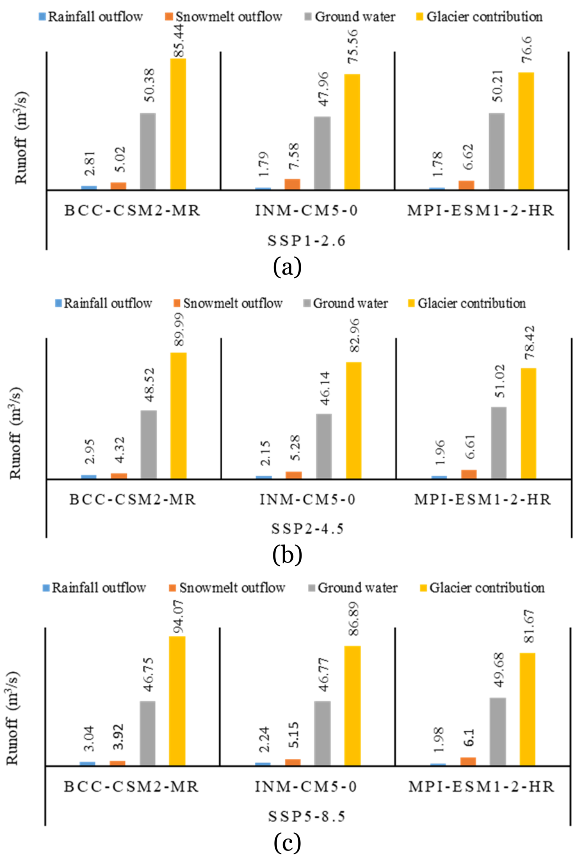

Fig. 12 Runoff contribution by different flow component during 2020-2070 under SSP1-2.6 (a) SSP2-4.5 (b) and SSP5-8.5 (c).

Table 8 Relative changes of streamflow in the Astore basin during the period of 2020-2070 compared to the period of 1990-2014

Climate Model	SSP1-2.6	SSP2-4.5	SSP5-8.5
BCC-CSM2-MR	-3%	-2%	-1%
INM-CM5-0	-11%	-9%	-6%
MPI-ESM1-2-HR	-9%	-8%	-7%

5 Conclusions

In this study, the hydrological response of the Astore River basin was examined and attributed to climatic variables of selected GCMs under different SSPs scenarios by applying the statistical tests and UBC watershed model (WM). The following conclusions have been drawn by analyzing the results:

- The future projections of precipitation showed a rise under the SSP1-2.6, SSP2-4.5, and SSP5-8.5 scenarios of the examined climate models, with the exception of BCC-CSM2-MR under SSP5-8.5. By the end of the 2070s, there were significant seasonal variations in the projected precipitation particularly in summer and winter seasons. Moreover, the anticipated temperature (T_{max} and T_{min}) over the Astore Basin indicated an upward trend.
- The change in temperature over Astore basin is expected to rise by −0.66°C-0.50°C, −0.14°C -0.87°C, and 0.05°C-1.16°C with respect to the SSP1-2.6, SSP2-4.5, and SSP5-8.5 scenarios. Consequently, the hydrologic regime of the Astore River basin may be significantly affected by acceleration of glacier melting.
- Projected streamflows for the period of 2020-2070 suggested an increase in the catchment. However, the contributions of snowmelt and groundwater to streamflows continued to decrease, while the contribution of rainfall and glacier melts remained to increase following SSP1-2.6, SSP2-4.5 and SSP5-8.5. Additionally, the future streamflow changes relative to the period of 1990-2014 indicated a decrease of up to 3%-11%, 2%-9%, and 1%-7% by SSP1-2.6, SSP2-4.5, and SSP5-8.5, respectively.

Based on the results and analyses mentioned earlier, it can be concluded that the average annual streamflow in the Astore River will decline by the end of 2070's as compared to 1990-2014 because of higher increase in temperature variables and less increase in precipitation. Hence, it is crucial to examine how the hydrology of the Astore basin will react to climate change. These findings should be adopted to manage the water storage and resources in Pakistan's Upper Indus Basin effectively, which includes Diamer-Basha dam and other planned reservoirs.

Acknowledgement

The authors are grateful to the Centre of Excellence in Water Resource Engineering, UET, Lahore and College of Engineering, IT and Environment, Charles Darwin University, Australia for support in conducting this study. The authors are also thankful to Pakistan Meteorological Department (PMD) and Water and Power Development Authority (WAPDA), Pakistan to provide the observed meteorological and hydrological data used in the study.

Author Contribution

All authors contributed to the study conception and design. Material preparation, data collection and analysis were performed by Zeshan Ali, Mudassar Iqbal and Ihsan Ullah Khan. The first draft of the manuscript was written by Zeshan Ali and all authors commented on previous versions of the manuscript. All authors read and approved the final manuscript.

Ethics Declaration

Data Availability: The spatial data used in this study including elevation, land use and glaciers data is freely available and can be accessed from the websites given in data section of the manuscript. The climatic parameters and streamflow data is the property of Pakistan Meteorological Department (PMD) and Water and Power Development Authority (WAPDA), Pakistan, respectively and can be requested to these departments via official channels.

Conflict of Interest: The authors declare no conflicts of interest.

Open Access

This article is licensed under a Creative Commons Attribution 4.0 International License, which permits use, sharing, adaptation, distribution and reproduction in any medium or format, as long as you give appropriate credit to the original author(s) and the source, provide a link to the Creative Commons license, and indicate if changes were made. The images or other third party material in this article are included in the article's Creative Commons license, unless indicated otherwise in a credit line to the material. If material is not included in the article's Creative Commons license and your intended use is not permitted by statutory regulation or exceeds the permitted use, you will need to obtain permission directly from the copyright holder. To view a copy of this license, visit http://creativecommons.org/licenses/by/4.0/.

Funding note: Open Access funding enabled and organized by CAUL and its Member Institutions

References

Adnan M, Liu S, Saifullah M, et al (2022) Spatiotemporal variations in runoff and runoff components in response to climate change in a glacierized subbasin of the Upper Indus Basin, Pakistan. Front Earth Sci 10:1-20. https://doi.org/10.3389/feart.2022.970349

Adnan M, Nabi G, Kang S, et al (2017) Snowmelt runoff modelling under projected climate change patterns in the Gilgit river basin of northern Pakistan. Polish J Environ Stud 26(2):525-542. https://doi.org/10.15244/pjoes/66719

Afshan N, Khalid A, Iqbal S, et al (2009) Puccinia subepidermalis sp. nov. and new records of rust fungi from Fairy Meadows, Northern Pakistan. Mycotaxon 110: 173-182. https://doi.org/10.5248/110.173

Akhtar N, Ahmad N, Booij MJ (2008) The impact of climate change on the water resources of Hindukush-Karakorum-Himalaya region under different glacier coverage scenarios. J Hydrol 355(1-4): 148-163. https://doi.org/10.1016/j.jhydrol.2008.03.015

Alhaji UU, Yusuf AS, Edet CO, et al. (2018) Trend analysis of temperature in Gombe State using Mann Kendall trend test. J Sci Res Reports 20(3):1-9. https://doi.org/10.9734/jsrr/2018/42029

Ali AF, Xiao CD, Zhang XP, et al. (2018) Projection of future streamflow of the Hunza River Basin, Karakoram Range (Pakistan) using HBV hydrological model. J Mt Sci 15:2218-2235. https://doi.org/10.1007/s11629-018-4907-4

Almazroui M, Islam MN, Saeed F, et al. (2021) Projected changes in temperature and precipitation over the United States, Central America, and the Caribbean in CMIP6 GCMs. Earth Syst Environ 5:1-24. https://doi.org/10.1007/s41748-021-00199-5

Arfan M, Lund J, Hassan D, et al. (2019) Assessment of spatial and temporal flow variability of the Indus River. Resources 8(2): 103. https://doi.org/10.3390/resources80201031

Atif I, Iqbal J, Su LJ (2019) Modeling hydrological response to climate change in a data-scarce glacierized high mountain Astore basin using a fully distributed TOPKAPI model. Climate 7(11): 127. https://doi.org/10.3390/cli7110127

Ayub S, Akhter G, Ashraf A, Iqbal M (2020) Snow and glacier melt runoff simulation under variable altitudes and climate scenarios in Gilgit River Basin, Karakoram region. Model Earth Syst Environ 6:1607-1618. https://doi.org/10.1007/s40808-020-00777-y

Baig S, Sayama T, Takara K (2021) Hydrological modeling of the astore river basin, pakistan, by integrating snow and glacier melt processes and climate scenarios. J Disaster Res 16(8):1197-1206. https://doi.org/10.20965/jdr.2021.p1197

Beckers J, Smerdon B, Wilson M (2009) Review of hydrologic models for forest management and climate change applications in British Columbia and Alberta. FORREX - Forum for Research and Extension in Natural Resources, Kamloops, Canada. 13(1):35- 44.

Berg P, Feldmann H, Panitz HJ (2012) Bias correction of high resolution regional climate model data. J Hydrol 448-449:80-92. https://doi.org/10.1016/j.jhydrol.2012.04.026

Bontemps S, Defourny P, Bogaert E Van, et al. (2011) GLOBCOVER 2009 Products Description and Validation Report. ESA Bull 136:53.

Chiew FHS, Kirono DGC, Kent DM, et al. (2010) Comparison of runoff modelled using rainfall from different downscaling methods for historical and future climates. J Hydrol 387(1-2):10-23. https://doi.org/10.1016/j.jhydrol.2010.03.025

Chisanga C, Phiri E, Chinene V (2017) Statistical bias correction of Fifth Coupled Model Intercomparison Project data from the CGIAR Research Program on climate change, Agriculture and Food Security - Climate Portal for Mount Makulu, Zambia. Br J Appl Sci Technol 21(4):1-16. https://doi.org/10.9734/bjast/2017/33531

Cook BI, Mankin JS, Marvel K, et al. (2020) Twenty-first century drought projections in the CMIP6 forcing scenarios. Earth's Futur 8(6). https://doi.org/10.1029/2019EF001461

Eyring V, Bony S, Meehl GA, et al. (2016) Overview of the Coupled Model Intercomparison Project Phase 6 (CMIP6) experimental design and organization. Geosci Model Dev 9(5):1937-1958. https://doi.org/10.5194/gmd-9-1937-2016

Fang G, Yang J, Chen Y, et al. (2015) Climate change impact on the hydrology of a typical watershed in the Tianshan Mountains. Adv Meteorol 2015: 1-10. https://doi.org/10.1155/2015/960471

Farhan SB, Zhang Y, Ma Y, et al. (2015) Hydrological regimes under the conjunction of westerly and monsoon climates: a case investigation in the Astore Basin, Northwestern Himalaya. Clim Dyn 44:3015-3032. https://doi.org/10.1007/s00382-014-2409-9

Garee K, Chen X, Bao A, et al. (2017) Hydrological modeling of the upper indus basin: A case study from a high-altitude glacierized catchment Hunza. Water (Switzerland) 9(1):1-20. https://doi.org/10.3390/w9010017

Gocic M, Trajkovic S (2013) Analysis of changes in meteorological variables using Mann-Kendall and Sen's slope estimator statistical tests in Serbia. Glob Planet Change 100:172-182. https://doi.org/10.1016/j.gloplacha.2012.10.014

Hassan J, Kayastha RB, Shrestha A, et al. (2017) Predictions of future hydrological conditions and contribution of snow and ice melt in total discharge of Shigar River Basin in Central Karakoram, Pakistan. Sci Cold Arid Reg 9(6):511-524. https://doi.org/10.3724/SP.J.1226.2017.00511

Hayat H, Akbar TA, Tahir AA, et al. (2019) Simulating current and future river-flows in the snowmelt-runoff model and RCP scenarios. Water 11(4): 1-19. https://doi.org/10.3390/w11040761

Ikram F, Afzaal M, Bukhari SAA, Ahmed B (2016) Past and future trends in frequency of heavy rainfall events over Pakistan. Pakistan J Meteorol 12(24):57-78.

Immerzeel WW, van Beek LPH, Konz M, et al. (2012) Hydrological response to climate change in a glacierized catchment in the Himalayas. Clim Change 110:721-736. https://doi.org/10.1007/s10584-011-0143-4

IPCC (2021) Summary for Policymakers. In: Lee H, Calvin K, Dasgupta D, et al (eds.), Synthesis Report of the IPCC Sixth Assessment Report (AR6): The Physical Science Basis. Contribution of Working Group I to the Sixth Assessment Report of the Intergovernmental Panel on Climate Change. Cambridge University Press, Cambridge, United Kingdom and New York, NY, USA. https://doi.org/10.3410/f.740620545.793587812

Iqbal M, Wen J, Masood M, et al. (2022) Impacts of climate and land-use changes on hydrological processes of the source region of Yellow River, China. Sustainability 14 (22). https://doi.org/10.3390/su142214908

Iqbal M, Wen J, Wang X, et al. (2018) Assessment of air temperature trends in the source region of Yellow River and its sub-basins, China. Asia-Pacific J Atmos Sci 54:111-123. https://doi.org/10.1007/s13143-017-0064-x

Kendall MG (1975) Rank correlation methods, Griffin Press, London, UK, 4th edition.

Khan AJ, Koch M (2021) Generation of a long-term daily gridded precipitation dataset for the Upper Indus Basin (UIB) through temporal Reconstruction, Correction & Informed Regionalization-"ReCIR". Int Soil Water Conserv Res 9(3): 445-460. https://doi.org/10.1016/j.iswcr.2021.01.005

Khan SA, Ashiq M, Gabriel HF (2014) Assessment of flows in a glaciated region-Shigar River Basin , Pakistan. Tech Journal, Univ Eng Technol Taxila 19(1):38-50.

Kim YH, Min SK, Zhang X, et al. (2020) Evaluation of the CMIP6 multi-model ensemble for climate extreme indices. Weather Clim Extrem 29. https://doi.org/10.1016/j.wace.2020.100269

Kreienkamp F, Lorenz P, Geiger T (2020) Statistically downscaled CMIP6 projections show stronger warming for Germany. Atmosphere (Basel) 11(11): 1-19. https://doi.org/10.3390/atmos11111245

Latif Y, Yaoming M, Yaseen M (2018) Spatial analysis of precipitation time series over the Upper Indus Basin. Theor Appl Climatol 131:761-775. https://doi.org/10.1007/s00704-016-2007-3

Loukas A, Vasiliades L (2014) Streamflow simulation methods for ungauged and poorly gauged watersheds. Nat Hazards Earth Syst Sci 14:1641-1661. https://doi.org/10.5194/nhess-14-1641-2014

Mann HB (1945) Nonparametric test against trend. Econometrica 13(3): 245-259. https://doi.org/10.2307/1907187

Marotzke J, Jakob C, Bony S, et al. (2017) Climate research must sharpen its view. Nature Clim Change 7:89-91. https://doi.org/10.1038/nclimate3206

Masood M, Shakir AS, Azhar AH, et al. (2020) Assessment of real time, multi-satellite precipitation products under diverse climatic and topographic conditions. Asia-Pacific J Atmos Sci 56:577-591. https://doi.org/10.1007/s13143-019-00166-1

Meinshausen M, Nicholls ZRJ, Lewis J, et al. (2020) The shared socio-economic pathway (SSP) greenhouse gas concentrations and their extensions to 2500. Geosci Model Dev 13(8):3571-3605. https://doi.org/10.5194/gmd-13-3571-2020

Mishra V, Bhatia U, Tiwari AD (2020) Bias-corrected climate projections for South Asia from Coupled Model Intercomparison Project-6. Sci Data 7:1-13. https://doi.org/10.1038/s41597-020-00681-1

Moriasi DN, Arnold JG, Van Liew MW, et al. (2007) Model evaluation guidelines for systematic quantification of accuracy in watershed simulations. Am Soc Agric Biol Eng 50(3): 885-900. https://doi.org/10.13031/2013.23153

Moss R, Babiker M, Brinkman S, et al. (2008) Towards new scenarios for analysis of emissions, climate change, impacts, and response strategies : IPCC Expert Meeting report : 19-21 September, 2007, Noordwijkerhout, the Netherlands. Intergovernmental Panel on Climate Change https://doi.org/10.1017 /cb09 780511546013.004

Naeem UA, Hashmi HN, Shamim MA, et al. (2012) Flow variation in Astore River under assumed glaciated extents due to climate change. Pak J Engg & Appl Sci 11:73-81.

Naeem UA, Habib-ur-Rehman, Hashmi HN, et al. (2015) Ranking sensitive calibrating parameters of UBC Watershed Model. KSCE J Civ Eng 19:1538-1547. https://doi.org/10.1007/s12205-015-0515-9

O'Neill BC, Kriegler E, Riahi K, et al. (2014) A new scenario framework for climate change research: The concept of shared socioeconomic pathways. Clim Change 122:387-400. https://doi.org/10.1007/s10584-013-0905-2

Pokhrel I, Kalra A, Rahaman MM, et al. (2020) Forecasting of future flooding and risk assessment under CMIP6 climate projection in Neuse River, North Carolina. Forecasting 2(3):323-345. https://doi.org/10.3390/forecast2030018

Quick MC, Pipes A (1977) U.B.C. watershed model. Hydrol Sci Bull 22:153-161. https://doi.org/10.1080/02626667709491701

Quick MC, Pipes A (1976) A Combined snowmelt and rainfall runoff model. Can J Civ Eng 3(3):449-460. https://doi.org/10.1139/l76-045

Quick MC (1995) University of British Columbia Watershed Model Manual Version 4.0., Department of Civil Engineering, The University of British Columbia Vancouver Campus, B.C., Canada.

Salma S, Rehman S, Shah MA (2012) Rainfall trends in different climate zones of Pakistan. Pakistan J Meteorol 9(17):37-47.

Salmi T, Määttä A, Anttila P, et al. (2002) Detecting trends of annual values of atmospheric pollutants by the Mann-Kendall test and Sen's slope estimates: The Excel template application MAKESENS. Publications on Air Quality No. 31, Report code FMI-AQ-31, Finnish Meteorological Institute, 35 pp.

Sen PK (1968) Estimates of the regression coefficient based on Kendall's Tau. J Am Stat Assoc 63(324):1379-1389. doi/abs/10.1080/01621459.1968.10480934

Shadmani M, Marofi S, Roknian M (2012) Trend analysis in reference evapotranspiration using Mann-Kendall and Spearman's Rho tests in arid regions of Iran. Water Resour Manag 26:211-224. https://doi.org/10.1007/s11269-011-9913-z

Shafeeque M, Luo Y (2021) A multi-perspective approach for selecting CMIP6 scenarios to project climate change impacts on glacio-hydrology with a case study in Upper Indus river basin. J Hydrol 599: 126466. https://doi.org/10.1016/j.jhydrol.2021.126466

Shakir AS, Habib -ur- Rehman, Ehsan S (2010) Climate change impact on river flows in Chitral Watershed. Pakistan J Eng Appl Sci 7:12-23.

Shifteh Some'e B, Ezani A, Tabari H (2012) Spatiotemporal trends and change point of precipitation in Iran. Atmos Res 113:1-12. https://doi.org/10.1016/j.atmosres.2012.04.016

Shrestha M, Acharya SC, Shrestha PK (2017) Bias correction of climate models for hydrological modelling - are simple methods still useful? Meteorol Appl 24(3):531-539. https://doi.org/10.1002/met.1655

Sleziak P, Výleta R, Hlavčová K, et al. (2021) A hydrological modeling approach for assessing the impacts of climate change on runoff regimes in Slovakia. Water (Switzerland) 13(23):1-21. https://doi.org/10.3390/w13233358

Syed Z, Ahmad S, Dahri ZH, et al. (2022) Hydroclimatology of the Chitral River in the Indus Basin under changing climate. Atmosphere 13(2): 1-20. https://doi.org/10.3390/atmos13020295

Tahir AA, Adamowski JF, Chevallier P, et al. (2016) Comparative assessment of spatiotemporal snow cover changes and hydrological behavior of the Gilgit, Astore and Hunza River basins (Hindukush-Karakoram-Himalaya region, Pakistan). Meteorol Atmos Phys 128:793-811. https://doi.org/10.1007/s00703-016-0440-6

Tahir AA, Chevallier P, Arnaud Y, et al. (2011) Snow cover dynamics and hydrological regime of the Hunza River basin, Karakoram Range, Northern Pakistan. Hydrol Earth Syst Sci 15(7):2275-2290. https://doi.org/10.5194/hess-15-2275-2011

Usta DFB, Teymouri M, Chatterjee U (2022a) Assessment of temperature changes over Iran during the twenty-first century using CMIP6 models under SSP1-26, SSP2-4.5, and SSP5-8.5 scenarios. Arab J Geosci 15:416. https://doi.org/10.1007/s12517-022-09709-9

Usta DFB, Teymouri M, Chatterjee U, et al. (2022b) Projections of atmospheric changes over Iran in 2014-2050 using the CMIP6-HighResMIP experiment. Arab J Geosci 15:1-18. https://doi.org/10.1007/s12517-022-10639-9

Usta DFB, Teymouri M, Chatterjee U, et al. (2022c) Temperature projections over Iran during the twenty-first century using CMIP5 models. Model Earth Syst Environ 8:749-760. https://doi.org/10.1007/s40808-021-01115-6

Wang S, Ding Y, Iqbal M (2017) Defining runoff indices and analyzing their relationships with associated precipitation and temperature indices for Upper River basins in the Northwest Arid region of China. Water (Switzerland) 9(8). https://doi.org/10.3390/w9080618

Waseem M, Ajmal M, Ahmad I, et al. (2021) Projected drought pattern under climate change scenario using multivariate analysis. Arab J Geosci 14(544):1-13. https://doi.org/10.1007/s12517-021-06860-7

Zhang Y, You Q, Chen C, et al. (2016) Impacts of climate change on streamflows under RCP scenarios: A case study in Xin River Basin, China. Atmos Res 178-179:521-534. https://doi.org/10.1016/j.atmosres.2016.04.018

Zhang L, Karnauskas KB, Donnelly JP, et al. (2017) Response of the North Pacific tropical cyclone climatology to global warming: Application of dynamical downscaling to CMIP5 models. J Clim 30(4):1233-1243. https://doi.org/10.1175/JCLI-D-16-0496.1